

A Study of Different Antenna Models on the Performance of UAV-Based LoRa Communication Network Using Taguchi and ANOVA Methods

Mohamad Hazwan Mohd Ghazali¹, Kelvin Teoh¹ and Wan Rahiman^{1,2,3*}

¹*School of Electric & Electronic Engineering, Universiti Sains Malaysia Engineering Campus, 14300 Nibong Tebal, Pulau Pinang, Malaysia*

²*Cluster of Smart Port and Logistics Technology (COSPALT), Universiti Sains Malaysia Engineering Campus, 14300 Nibong Tebal, Pulau Pinang, Malaysia*

³*Daffodil Robotics Lab, Department of Computer Science and Engineering, Daffodil International University, Dhaka, Bangladesh*

ABSTRACT

In a UAV-based LoRa communication network, one critical aspect that requires careful consideration is the weight applied to the UAV, which can be affected by the choice of antenna and the size of the power source utilized to operate the LoRa device. Therefore, in this study, the effects of different antenna models, transmitting powers (TP), and surrounding temperatures on the performance of LoRa are investigated under varying conditions. The other contributions of the paper include investigating the optimum LoRa configuration under different test scenarios and the correlation between TP and power consumption. Based on the Taguchi and ANOVA analysis, the optimum LoRa configuration in terms of packet delivery rate (PDR) for a 1 km direct line-of-sight scenario is TP = 15 dBm, antenna model = 5 dBi antenna, and surrounding temperature = 34°C. With the optimum setting, the power consumption was reduced to approximately 168.4 mW, and 3789 times more data transmission can be achieved compared to the default parameter. Therefore, a smaller power source can prolong the UAV flight time.

Keywords: Antenna, drone, LoRa, power consumption, wireless communication

ARTICLE INFO

Article history:

Received: 11 December 2023

Accepted: 16 April 2024

Published: 21 February 2025

DOI: <https://doi.org/10.47836/pjst.33.2.01>

E-mail addresses:

hazwan_ghazali@yahoo.com (Mohamad Hazwan Mohd Ghazali)

ttk.kelvin@gmail.com (Kelvin Teoh)

wanrahiman@usm.my (Wan Rahiman)

*Corresponding author

INTRODUCTION

LoRa has been increasingly utilized worldwide, where the number of countries deploying long-range wide-area networks (LoRaWAN) is nearly 150 (Edward et al., 2020). The commercial growth of LoRa is

due to its advantages, which include offering long-range (at the scale of kilometers), low power, and secure data transmission for Internet of Things (IoT) applications. However, LoRa requires a trade-off between communication range and data rates. The data rate has to be reduced to achieve a higher communication range and vice versa. LoRa is based on chirp spread spectrum (CSS) modulation, where chirps are signals that have a fluctuating frequency over time. This modulation spreads the data along the bandwidth using a Spreading Factor (SF), which will generate a signal resilient against noise and other interference.

Using UAVs can expand the potential of LoRa in data collection and transmission, and this UAV-based LoRa can be classified into LoRa node and LoRa gateway (Ghazali et al., 2021). It is made possible thanks to the high maneuverability, customizability, and pervasiveness of UAVs (Wang et al., 2021). For instance, a UAV equipped with relevant sensors and a LoRa device can act as a LoRa node and be deployed in locations with difficult access to monitor the quality of the air or traffic and transmit the information to the base station (J. Liu et al., 2020; S. Liu et al., 2020; Trasvina-Moreno et al., 2017). As a LoRa gateway, in some of the precision agriculture and livestock farming applications, a UAV carrying a LoRa device will fly above the LoRa nodes on the ground to collect the data and relay it to the base station (Caruso et al., 2021 Vlasceanu et al., 2019; Behjati et al., 2021; Zorbas & O'Flynn, 2019). Other advantages of UAV-based LoRa communication include its high flexibility, line-of-sight transmission, and reduced computing pressures and computation delay (Lu et al., 2022; Ding et al., 2022). However, there is a trade-off between communication rate and bit rate, in which increasing the bit rate will reduce the communication range—also, the higher the bit rate, the longer the duration of data transmission. LoRa's communication performance also depends on tuning several PHY settings, such as the coding rate (CR), SF, bandwidth (BW), and transmit power (TP).

Many researchers have conducted various studies to evaluate the performance of the LoRa communication network. Faber et al. (2020) and Sanchez-Iborra et al. (2018) assessed the reliability of LoRa in terms of packet error rate (PER) and packet delivery rate (PDR), respectively, under urban and suburban scenarios. Meanwhile, different PHY settings (CR, BW, and SF) have been utilized by Yim et al. (2018) to determine their effects on the LoRa's RSSI and PDR. By applying the LoRa shield based on the Semtech SX1276 chip that works on the 915 MHz band, they also studied the influence of different antenna placements on the LoRa performance. It was discovered that BW had the lowest impact on the LoRa performance compared to CR and SF, and raising the antenna from 0 to 1 m can drastically improve the LoRa signal. Similar work has been conducted by Cattani et al. (2017), utilizing the HopeRF RFM95 LoRa device that operates in the 868 MHz band. Additionally, they investigated the impacts of surrounding temperatures on the LoRa's packet reception rate (PRR). The worst PRR was registered at a temperature of 60°C.

Regarding the TP setting, few researchers have conducted a comprehensive study on this matter. Liang et al. (2020) analyzed the effects of different TPs (20, 17, 14, 10 dBm) and payload length on the LoRa performance in terms of PDR and round-trip time in an indoor environment. A LoRa module based on the Semtech SX1278 chip with a 433 MHz band was used in this study. Experimental results showed that the different TPs had minimal effects on the RTT, and using the lowest setting (10 dBm) could still yield satisfactory PDR. Similarly, (Wang et al., 2017) an investigation was conducted to determine the correlation between different TPs (20, 11, 2 dBm) and the LoRa's packet loss rate. The PLR increased from 0% to 68% when the TP was changed from 20 dBm to 2 dBm. Petajajarvi et al. (2017) evaluated the performance of LoRa in terms of PDR and RSSI using the TP of 14 dBm. Experimental results demonstrated that 60% of the packets could be successfully delivered at a 30 km communication range using the highest spreading factor of 12 and TP of 12 dBm.

As observed in the reviewed works, most of the previous literature analyzed the influence of several PHY settings on the LoRa performance in terms of RSSI, PLR, and PDR parameters. The experimental works have been conducted in various environments, ranging from urban to rural areas. It is commonly understood that UAVs have a limited operational time. Therefore, in a UAV-based LoRa communication network, selecting the best LoRa configuration is crucial to achieving the optimum results without excessively compromising power consumption and flight time. This is what motivates us to perform this study. The key advantage of this work is that, to the best of our knowledge, no literature investigates the impact of different antenna models on LoRa's performance. In addition, compared to existing studies, this work analyzes the correlation between TP and power consumption. The main contributions of this study are as follows:

1. The effects of different antenna models, TPs, and surrounding temperatures on the LoRa RSSI and PDR are investigated.
2. The reliability of LoRa under different test scenarios is presented.
3. The correlation between TP and power consumption is analyzed.
4. The optimized LoRa's configuration for different test scenarios is identified and discussed.

METHODOLOGY

Taguchi Method

Careful planning of the experiment is vital if the full benefits of the experimental methods are to be realized. The Taguchi approach is one of the very useful DOE methods for determining the optimized configuration of different parameters for the best performance. Opposite to other DOE techniques, such as full factorial analysis and response surface

methodology (RSM), the Taguchi approach minimizes the number of experimental runs to a reasonable one in terms of cost and time, using orthogonal arrays (Davis & Pretesh, 2018). Although the number of experiments is reduced, the output still contains the most information. While the RSM method also reduces the number of experiments, the Taguchi method requires fewer experiments than the RSM method to obtain optimum findings (Said et al., 2013). The Taguchi method is also more robust than the RSM technique. This study applied the Taguchi technique to determine the optimized LoRa configuration on the PDR and RSSI and obtain the contribution ratios and order of importance for each parameter.

The factors and levels used in the Taguchi analysis are listed in Table 1. The TP parameter has more levels than other factors due to its high selection choice. Out of the 19 different values (5 to 23 dBm), it is not convincing to select only three levels to determine the optimum TP. Besides, there is limited information regarding the TP used in previous studies. The antenna chosen is based on the widely used ones and must be light enough for the drone to carry. Three different surrounding temperatures represent three distinct environments at the test location. Specifically, a temperature of 27°C indicates the morning period from 8 am to 10 am, a temperature of 31°C indicates the evening period from 5 pm to 7 pm, and a temperature of 34°C indicates the afternoon period from 12 pm to 2 pm. In this research, the L18 Taguchi orthogonal array is chosen and presented in the experimental setup.

Table 1
Factors and levels used in the experiment

Factor	Level 1	Level 2	Level 3	Level 4	Level 5	Level 6
TP (A)	5 dBm	10 dBm	15 dBm	18 dBm	20 dBm	23 dBm
Antenna model (B)	2 dBi	5 dBi	8 dBi			
Surrounding temperature (C)	27°C	31°C	34°C			

The Taguchi analysis utilizes the signal-to-noise (S/N) ratio as a performance indicator to optimize the response variable against variations in noise factors. S/N ratio can be defined as the ratio of the mean (signal) to the standard deviation (noise) (Ginting & Tambunan, 2018). Taguchi has suggested many S/N ratios, but the three most commonly used are smallest-is-best (SB), largest-is-best (LB), and nominal-is-best (NB). This study selected the SB and LB S/N ratios because minimum RSSI and maximum PDR were desired. In practical application, a minimum RSSI is desired, where an RSSI of close to 0 means the received signal is of high quality. However, in Taguchi analysis, the response data cannot be negative; thus, the RSSI obtained from every transmission will be converted to a positive value. Hence, the SB S/N ratio is selected for RSSI response. Therefore, the S/N ratios are defined using the following Equations 1 and 2 (Bademlioglu et al., 2018):

$$\text{For SB, } S/N = -10\log\left(\frac{1}{n}\sum_{i=1}^n y_i^2\right) \quad [1]$$

$$\text{For LB, } S/N = -10\log\left(\frac{1}{n}\left(\frac{1}{\sum_{i=1}^n y_i^2}\right)\right) \quad [2]$$

where n represents the number of experimental trials, and y_i is the resulting value for the i th performance characteristics, which in this study is the PDR or average RSSI for each case.

Analysis of Variance (ANOVA)

After conducting the Taguchi analysis, the ANOVA analysis was carried out to determine the impact ratios of each parameter and to verify the results obtained from the Taguchi method. ANOVA is a statistical technique used to analyze variability in data measured under conditions defined by discrete factors. ANOVA has been widely used in various fields, such as psychology, biology, economics, and engineering, to name a few. In this study, the ANOVA analysis is adopted to analyze the effect level of each parameter on the LoRa's PDR and RSSI (Bademlioglu et al., 2018). In the ANOVA analysis, the sum of squares (SS), degrees of freedom (DOF), F values, mean of squares (MS), and parameters' impact ratios are computed as following Equations 3 to 7:

$$SS_{factor} = \frac{\beta_{factor,i}^2}{N} - \frac{(\sum \beta_i)^2}{n} \quad [3]$$

$$DOF_{factor} = k - 1 \quad [4]$$

$$V_{factor} = \frac{SS_{factor}}{DOF_{error}} \quad [5]$$

$$F_{factor} = \frac{V_{factor}}{V_{error}} \quad [6]$$

$$MS_{factor} = \frac{SS_{factor}}{DOF_{factor}} \quad [7]$$

The SS_{factor} represents the sums of squares due to factor, whereas β_i and $\beta_{factor,i}$ are the S/N ratio at the i th level of the factor and its sum, respectively (Equation 3). In Equation 4, the DOF_{factor} is the number of factors' DOF, and k represents the number of levels of the factor. The V_{factor} in Equation 5 represents the variance of the factor. For Equations 6 and 7, the F_{factor} is the factor's test value, V_{error} is the variance of the error, and MS_{factor} is the ratio of the SS values of each parameter to the DOF of each parameter. The most significant parameter and the parameter ranking obtained from the ANOVA analysis will be compared with the results from the Taguchi analysis.

EXPERIMENTAL SETUP

Hardware

Three omnidirectional antennas are used in this study, as shown in Figure 1, and their technical specifications are listed in Table 2. This study focuses exclusively on omnidirectional antennas, excluding horn and beam antennas from consideration due to their heavier weight, which renders them unsuitable for implementation with UAVs. These antennas are installed on the RFM LoRa shield, which integrates the RFM95W LoRa module. The LoRa shield is then attached to the Arduino UNO as a transmitter and powered

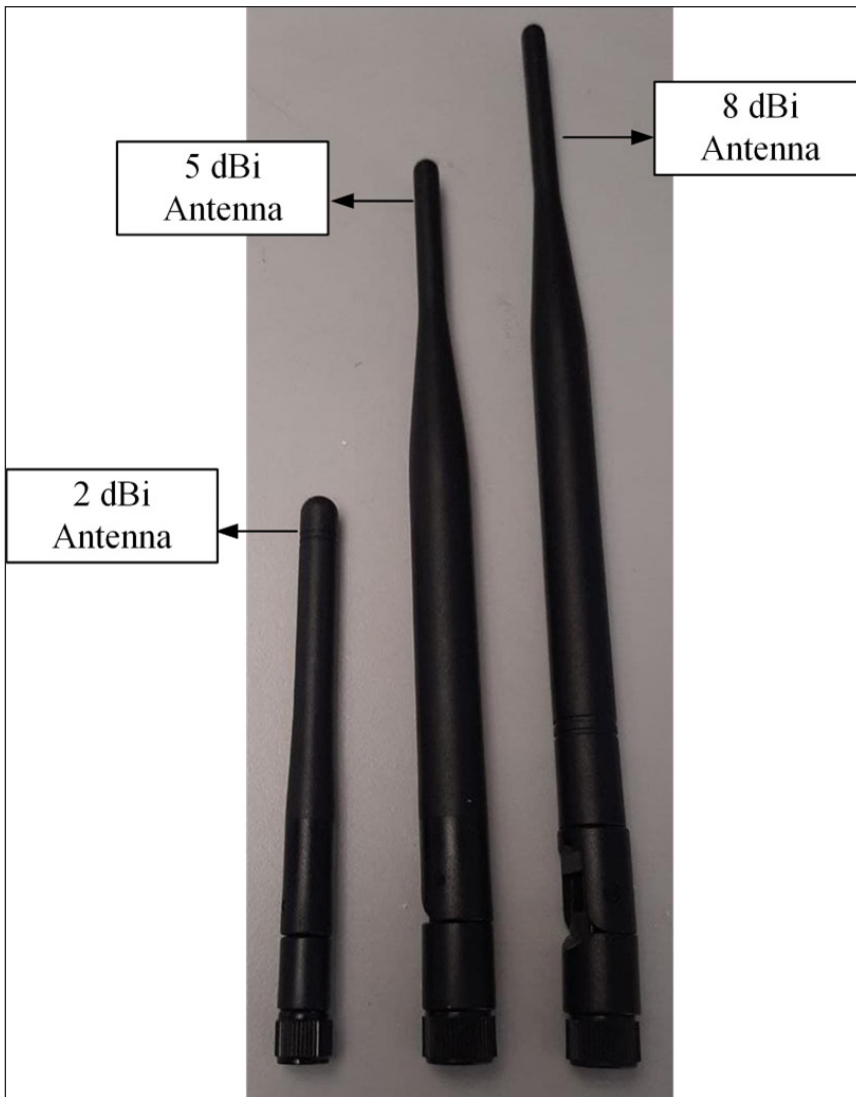


Figure 1. Three Omni-Directional Antennas with Different Antenna Gains used in this Experiment

by a 5000 mAh power bank (Figure 2). The UAV's center of gravity needs to be considered while mounting the antenna so that the UAV's stability is not disrupted during flying. The UAV used to carry the setup is the Storm Drone 8, an octocopter-type UAV with a maximum payload of 600 g, excluding the battery. The overall weight of the LoRa communication setup is approximately 168 g (8 dBi antenna = 19 g, LoRa shield = 25 g, Arduino UNO = 25 g, and power bank = 99 g), which is below the maximum payload of Storm Drone 8. Thus, the drone can deploy this experimental setup in the outdoor environment. For each LoRa configuration, the drone will fly with the LoRa transmitter up to approximately 3 m and transmit random integers to the LoRa receiver every 2.5 seconds. For each packet sent, we computed the PDR and RSSI.

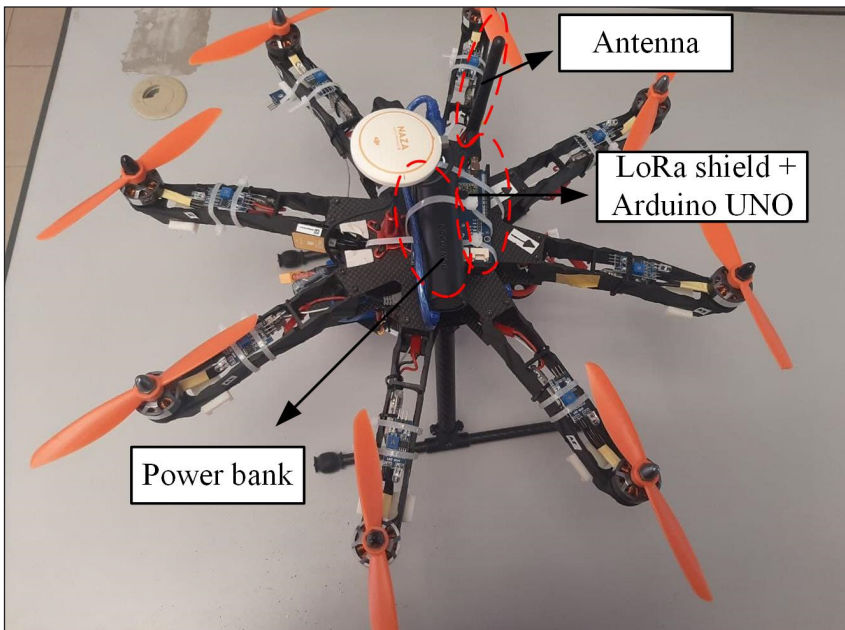


Figure 2. The Experimental Setup to Evaluate the Performance of UAV-Based LoRa Communication

Table 2
Technical Specifications of Three Antennas used in this Experiment

Specification	Antenna 1	Antenna 2	Antenna 3
Gain	2 dBi	5 dBi	8 dBi
Input Impedance	50 Ω	50 Ω	50 Ω
Antenna Length	10.9 cm	20 cm	24 cm
Frequency	915 MHz	915 MHz	915 MHz
Weight	10 g	16 g	19 g

Test Location

The experimental works are conducted in two different test locations, marked as Location A and B. Ban Pecah, located in Parit Buntar, Perak, Malaysia, is chosen as Location A because it can cater to the 1 km direct line-of-sight feature, as depicted in Figure 3(a). The areas inside Universiti Sains Malaysia, Penang, Malaysia, are chosen as Location B, as

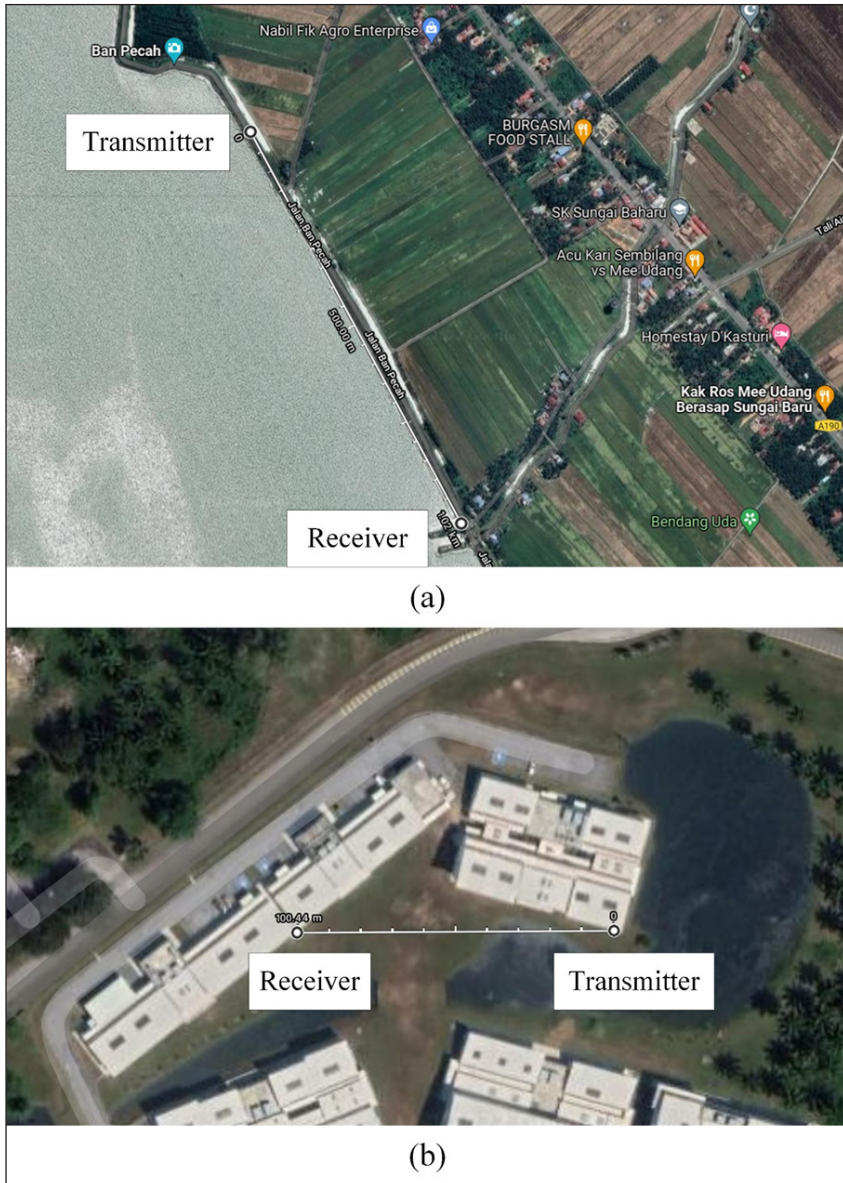


Figure 3. The Experimental Locations Used to Conduct the Study: (a) Location A in the Ban Pecah Area and (b) Location B in the University Area

shown in Figure 3(b), specifically for the 100 m direct line-of-sight scenario. Two different communication ranges are chosen because we want to determine whether the outputs behave the same in a short and long-range environment or not. As mentioned earlier, the optimum parameters for both communication ranges have been determined.

The correlation between TP and power consumption can be described based on the following Equation 8:

$$P_{mW} = 1 \text{ mW} \left(10^{\frac{P_{dBm}}{10}}\right) \quad [8]$$

where P_{mW} is the power in milliwatts (mW), and P_{dBm} represents the power in Decibel-milliwatts. The current drawn for each data transmission has to be calculated using Equation 9 to determine the number of packets that can be transmitted for a specific capacity of a power supply:

$$I = \sqrt{\frac{P_{mW}}{R}} \quad [9]$$

where I is the current drawn in milliampere (mA), and R is the resistance. Depending on the capacity of the power supply, the current value obtained will be used as a ratio to determine the maximum number of data transmissions.

RESULTS AND DISCUSSION

Tables 3 and 4 show the statistical analyses performed via the Taguchi technique for the 1 km and 100 m experimental scenarios. When data transmission is unsuccessful, the PDR is 0%. However, for the sake of Taguchi analysis, we computed the 0% PDR as 0.001%. We also assumed the worst possible RSSI, which is -146 dBm (according to the RFM LoRa Shield datasheet), for every unsuccessful LoRa communication. It can be seen that there are 18 cases with different levels of parameters (Tables 3 and 4). For instance, the PDR recorded for Trial 1 (Table 3) is 0.001% for a TP of 5 dBm, 2 dBi antenna model, and a surrounding temperature of 27°C. The higher the TP, the higher the tendency for successful LoRa communication (Figure 4). However, for the 2 dBi antenna model, the data can be transmitted only when the TP is set to 15 dBm. Also, Figures 4, 5 and Table 3 demonstrate that in the 1 km direct line-of-sight environment, the UAV-based LoRa communication is unsuccessful at all TPs and temperatures when the 8 dBi antenna model is applied. It might be due to an error in adjusting the position of the UAV to face the receiver, in which the UAV's position does not fall within the effective coverage angle of the 8 dBi antenna (Figure 6).

Table 3
PDRs and S/N Ratios for the L18 Orthogonal Array in a 1 km Test Scenario

Trial	Parameters			Results		S/N Ratio	
	A Level	B Level	C Level	PDR	Average RSSI	PDR	Average RSSI
1	5 dBm	2 dBi	27°C	0.001% (0%)	146 dBm (-146 dBm)	60	-43.287
2	5 dBm	5 dBi	31°C	25%	98 dBm (-98 dBm)	27.959	-39.825
3	5 dBm	8 dBi	34°C	0.001% (0%)	146 dBm (-146 dBm)	60	-43.287
4	10 dBm	2 dBi	27°C	0.001% (0%)	146 dBm (-146 dBm)	60	-43.287
5	10 dBm	5 dBi	31°C	75%	92 dBm (-92 dBm)	37.5	-39.276
6	10 dBm	8 dBi	34°C	0.001% (0%)	146 dBm (-146 dBm)	60	-43.287
7	15 dBm	2 dBi	31°C	85%	93 dBm (-93 dBm)	38.588	-39.37
8	15 dBm	5 dBi	34°C	100%	90 dBm (-90 dBm)	40	-39.085
9	15 dBm	8 dBi	27°C	0.001% (0%)	146 dBm (-146 dBm)	60	-43.287
10	18 dBm	2 dBi	34°C	90%	88 dBm (-88 dBm)	39.085	-38.89
11	18 dBm	5 dBi	27°C	99%	88 dBm (-88 dBm)	39.554	-38.89
12	18 dBm	8 dBi	31°C	0.001% (0%)	146 dBm (-146 dBm)	60	-43.287
13	20 dBm	2 dBi	31°C	100%	88 dBm (-88 dBm)	40	-38.89
14	20 dBm	5 dBi	34°C	100%	89 dBm (-89 dBm)	40	-38.99
15	20 dBm	8 dBi	27°C	0.001% (0%)	146 dBm (-146 dBm)	60	-43.287
16	23 dBm	2 dBi	34°C	100%	91 dBm (-91 dBm)	40	-39.181
17	23 dBm	5 dBi	27°C	100%	89 dBm (-89 dBm)	40	-38.99
18	23 dBm	8 dBi	31°C	0.001% (0%)	146 dBm (-146 dBm)	60	-43.287

Table 4

PDRs and S/N Ratios for the L18 Orthogonal Array in a 100 m Test Scenario

Trial	Parameters			Results		S/N Ratio	
	A Level	B Level	C Level	PDR	Average RSSI	PDR	Average RSSI
1	5 dBm	2 dBi	27°C	100%	72 dBm (-72 dBm)	40	-37.147
2	5 dBm	5 dBi	31°C	100%	66 dBm (-66 dBm)	40	-36.391
3	5 dBm	8 dBi	34°C	82%	95 dBm (-95 dBm)	38.276	-39.554
4	10 dBm	2 dBi	27°C	100%	66 dBm (66 dBm)	40	-36.391
5	10 dBm	5 dBi	31°C	100%	62 dBm (-62 dBm)	40	-35.848
6	10 dBm	8 dBi	34°C	93%	90 dBm (-90 dBm)	39.37	-39.085
7	15 dBm	2 dBi	31°C	100%	53 dBm (-53 dBm)	40	-34.486
8	15 dBm	5 dBi	34°C	100%	53 dBm (-53 dBm)	40	-34.486
9	15 dBm	8 dBi	27°C	96%	90 dBm (-90 dBm)	39.645	-39.085
10	18 dBm	2 dBi	34°C	100%	52 dBm (-52 dBm)	40	-34.32
11	18 dBm	5 dBi	27°C	100%	50 dBm (-50 dBm)	40	-33.979
12	18 dBm	8 dBi	31°C	100%	88 dBm (88 dBm)	40	-38.89
13	20 dBm	2 dBi	31°C	100%	50 dBm (-50 dBm)	40	-33.979
14	20 dBm	5 dBi	34°C	100%	48 dBm (-48 dBm)	40	-33.625
15	20 dBm	8 dBi	27°C	100%	85 dBm (-85 dBm)	40	-38.588
16	23 dBm	2 dBi	34°C	100%	50 dBm (-50 dBm)	40	-33.979
17	23 dBm	5 dBi	27°C	100%	46 dBm (-46 dBm)	40	-33.255
18	23 dBm	8 dBi	21°C	100%	83 dBm (-83 dBm)	40	-38.382

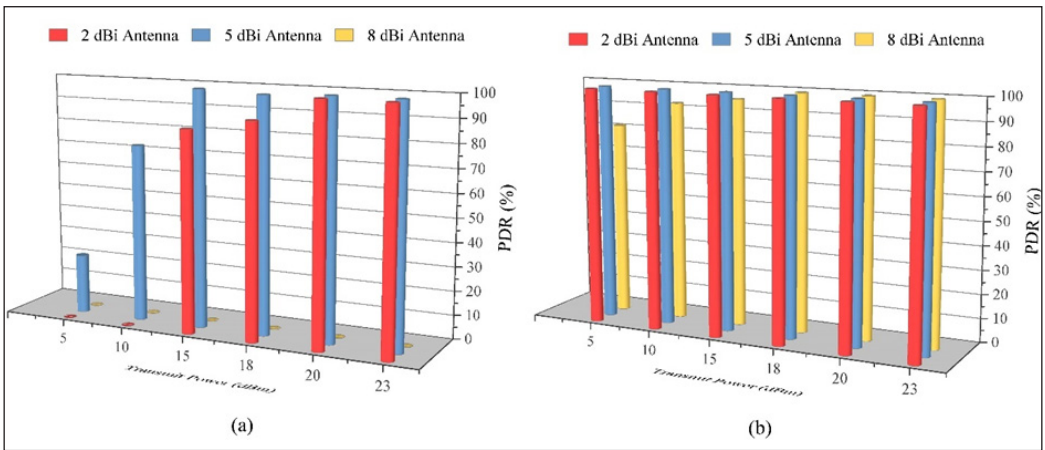


Figure 4. The PDRs Computed at Different TPs for 2 dBi, 5 dBi, and 8 dBi Antennas in (a) a 1 km Direct Line-of-Sight Environment and (b) a 100 m Direct Line-of-Sight Environment

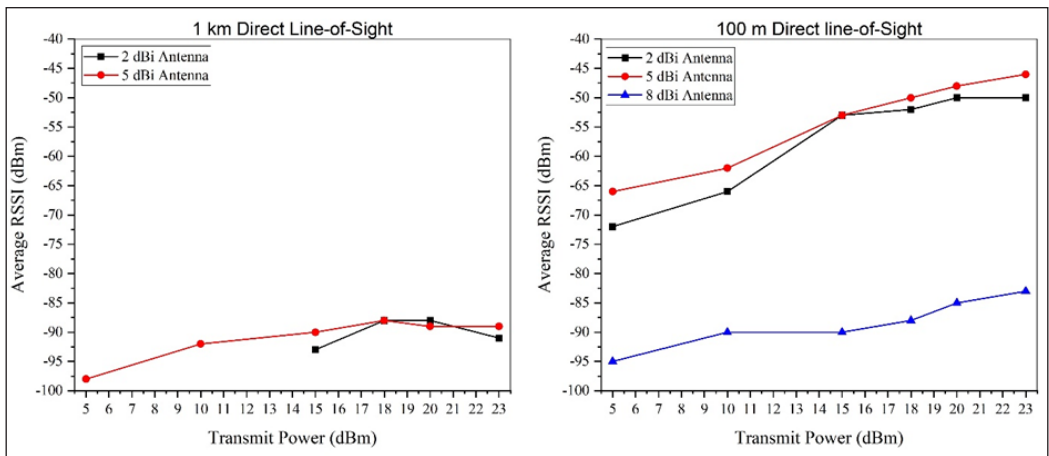


Figure 5. The Average RSSIs Computed at Different TPs for 2 dBi, 5 dBi, and 8 dBi Antennas in 1 km and 100 m Environments

In contrast to the 8 dBi antenna, the UAV-based LoRa communication with the 5 dBi antenna is successful at all experimental trials, though there are packet losses at the minimum TP. The LoRa communication using the 8 dBi antenna produced the worst PDR and average RSSI in 1 km and 100 m test scenarios, as depicted in Figures 3 and 4. The reason behind this is the narrow effective angle coverage of an 8 dBi antenna, compared to 2 dBi and 5 dBi antennas. The 2 dBi antennas can cover all 360 coverage angles, whereas 5 dBi antennas have a range of 40. As for the 8 dBi antenna, the effective coverage angle is between 25° and 30°. Thus, during the data collection process using the 8 dBi antenna, although the UAV that carried the LoRa transmitter was hovering, the effective angle

coverage was not static due to the slight movement of the UAV, which led to poor PDR and RSSI recorded. However, if the UAV's position is properly facing the 8 dBi receiver, the outcome could vary, and the 8 dBi antenna could potentially perform similarly or even better than the 5 dBi antenna.

For the 100 m direct line-of-sight test scenario, the LoRa communication is successful at every TP for all antenna models. However, for a 100% PDR, the TP must be set to 18 dBm if the 8 dBi antennas are used. The same results can be obtained for the 2 dBi and 5 dBi antennas, even if the minimum TP (5 dBm) is applied. In terms of RSSI, the 5 dBi antenna is the best choice for LoRa communication in the 100 m range, whereas if maximum PDR is desired, the 2 dBi antenna is sufficient.

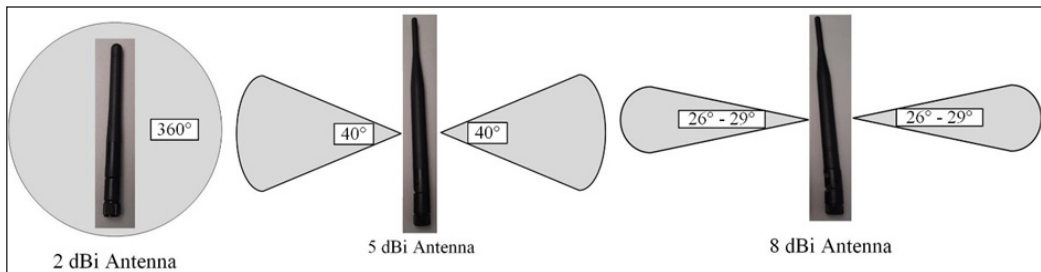


Figure 6. Effective Coverage Angles of Each LoRa Antenna

Average S/N ratios, contribution ratios, and parameter ranking on the PDR and average RSSI are computed using the Taguchi technique (Tables 5, 6, 7, and 8). The parameters are ranked based on the magnitude of the effect on PDR and average RSSI. It can be observed from Tables 5 to 8 that the antenna model is the most significant parameter on the PDR and average RSSI for both test scenarios. In contrast, the least significant parameter is

Table 5
Average S/N Ratio and Ranking of Parameters for the PDR in a 1 km Direct Line-of-Sight Scenario

Level	Parameters		
	A	B	C
1	-30.68	6.279	-14.411
2	-27.5	37.502	4.008
3	30.856	-47.67	6.514
4	6.213		
5	6.667		
6	6.667		
Delta	61.536	85.173	20.925
Contribution Ratio	36.71%	50.81%	12.48%
Rank	2	1	3

Table 6

Average S/N Ratio and Ranking of Parameters for the Average RSSI in a 1 km Direct Line-of-Sight Scenario

Level	Parameters		
	A	B	C
1	-42.13	-40.48	-41.84
2	-41.95	-39.13	-40.66
3	-40.58	-43.29	-40.40
4	-40.36		
5	-40.29		
6	-40.29		
Delta	1.84	4.16	1.43
Contribution Ratio	24.76%	55.99%	19.25%
Rank	2	1	3

Table 7

Average S/N Ratio and Ranking of Parameters for the PDR in a 100 m Direct Line-of-Sight Scenario

Level	Parameters		
	A	B	C
1	39.43	40	39.94
2	39.79	40	40
3	39.88	39.55	39.61
4	40		
5	40		
6	40		
Delta	0.57	0.45	0.59
Contribution Ratio	40.4%	31.9%	27.7%
Rank	1	2	3

Table 8

Average S/N Ratio and Ranking of Parameters for the Average RSSI in a 100 m Direct Line-of-Sight Scenario

Level	Parameters		
	A	B	C
1	-37.7	-35.05	-36.48
2	-37.11	-34.66	-36.40
3	-36.08	-39.01	-35.84
4	-35.73		
5	-35.36		
6	-35.46		
Delta	2.33	4.35	0.64
Contribution Ratio	31.8%	59.4%	8.8%
Rank	2	1	3

the surrounding temperature. Thus, the ranking orders of the impact of parameters on the average RSSI for both test scenarios are the same, which are antenna model > TP > surrounding temperature. For PDR, the ranking orders are determined as follows: antenna model > TP > surrounding temperature (for 1 km environment) and TP > antenna model > surrounding temperature (for 100 m environment).

Figures 7 and 8 demonstrate each parameter's effect on the PDR and average RSSI. The parameter is considered to strongly influence the output if there is a huge discrepancy between the maximum and minimum S/N ratios. Parameters that produce the highest S/N ratio will contribute to the desired optimum UAV-based LoRa configuration. Therefore, based on the Taguchi analysis, TP = 15 dBm, antenna model = 5 dBi antenna, and surrounding temperature = 34°C are determined as an optimum UAV-based LoRa configuration for maximum PDR (100%) in a 1 km direct line-of-sight scenario. As for the best average RSSI, the optimum configurations are TP = 20 dBm, antenna model = 5 dBi antenna, and surrounding temperature = 34°C. In addition, the worst LoRa configuration was found to be the TP = 5 dBm, antenna model = 8 dBi antenna, and surrounding temperature = 27°C, where LoRa communication was unsuccessful. As for the 100 m test scenario, the optimum LoRa configuration suggested by the Taguchi analysis is TP = 18 dBm, antenna model = 2 dBi antenna, and surrounding temperature = 31°C for the best PDR. However, from the experimental works, the minimum TP (5 dBm) can still yield 100% PDR when applied to the 2 dBi and 5 dBi antennas. For the best RSSI, the

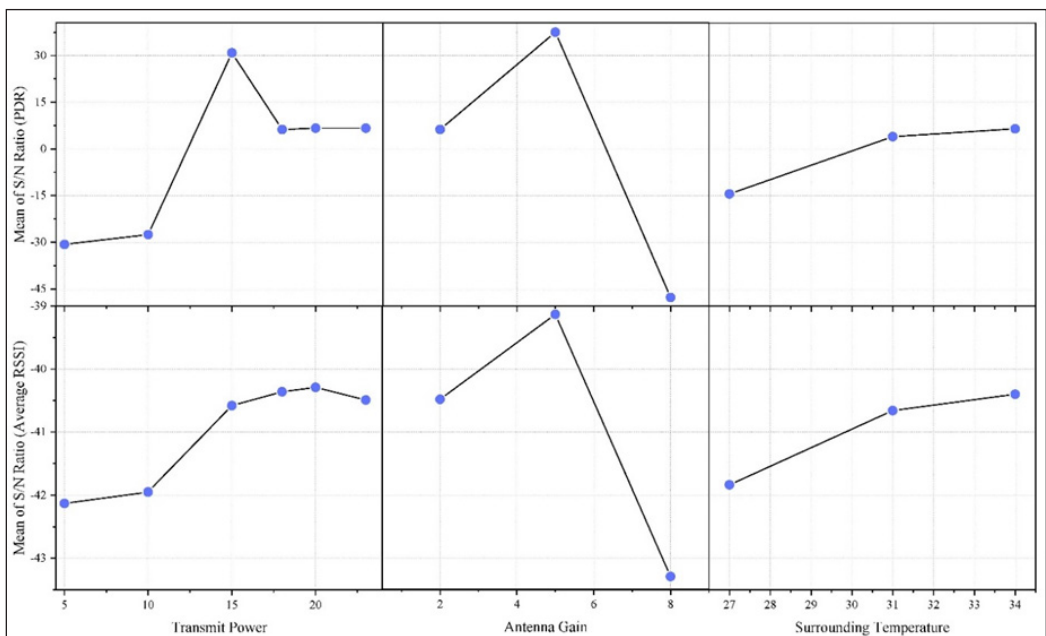


Figure 7. Effective of Each Parameter on the PDR and Average RSSI in a 1 km Direct Line-of-Sight Scenario

optimum LoRa configuration is determined as follows: TP = 20 dBm, antenna model = 5 dBi antenna, and surrounding temperature = 34°C. Minimum PDR and average RSSI are obtained under the following LoRa configuration: TP = 5 dBm, antenna model = 8 dBi antenna, and surrounding temperature = 34°C (for PDR) and 27°C (for average RSSI).

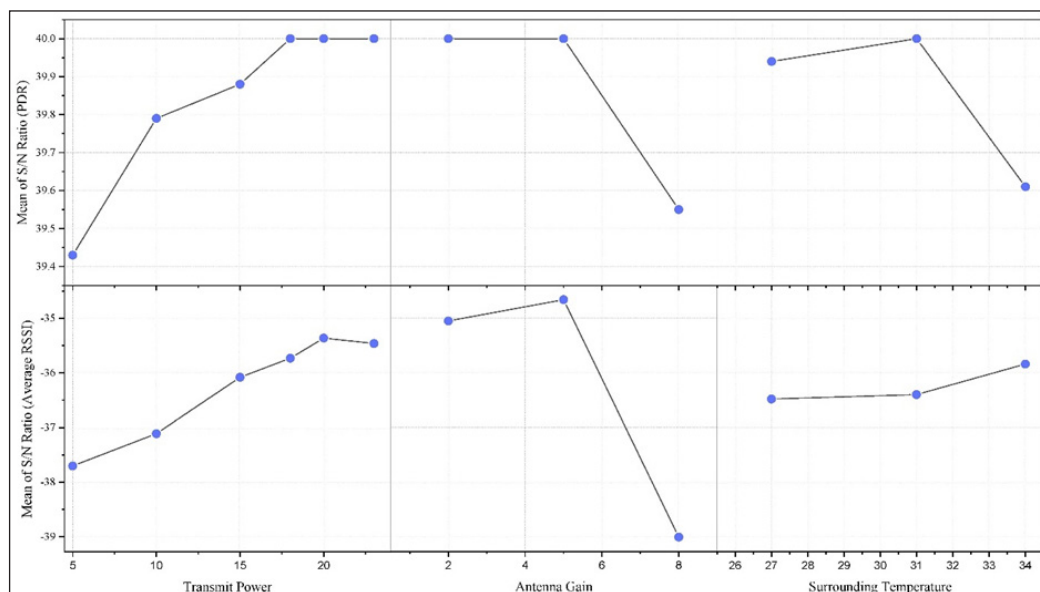


Figure 8. Effective of Each Parameter on the PDR and Average RSSI in a 100 m Direct Line-of-Sight Scenario

The ANOVA analysis was applied, and the outputs were obtained to verify the results of the Taguchi analysis (Tables 9, 10, 11, and 12). Based on the ANOVA tables, it can be seen that the most significant parameter on the PDR and average RSSI for 1 km test scenarios is the antenna gain, with an impact ratio of 75.96% and 82.92%, respectively. The order of importance of the parameters for the PDR and average RSSI is determined as antenna model > TP > surrounding temperature. These results are in agreement with the

Table 9
ANOVA Table for PDR in a 1 km Direct Line-of-Sight Scenario

Parameters	DOF	SS	MS	F	Contribution
TP	5	9657	1931.4	4.21	13.49%
AG	2	21744	10872	23.70	75.96%
ST	2	3019	1509.7	3.29	10.54%
Error	8	3669	458.7		
Total	17	38090			100%

TP = Transmit power, AG = Antenna gain, and ST = Surrounding temperature

results obtained from the Taguchi analysis. Although the contribution ratios computed from both analyses are slightly different, the ranking order of the parameters is still the same.

Table 10

ANOVA Table for Average RSSI in a 1 km Direct Line-of-Sight Scenario

Parameters	DOF	SS	MS	F	Contribution
TP	5	1270	634.9	4.08	10.96%
AG	2	9608	4804.1	30.87	82.92%
ST	2	1772	354.5	2.28	6.12%
Error	8	1245	155.6		
Total	17	13895			100%

TP = Transmit power, AG = Antenna gain, and ST = Surrounding temperature

Table 11

ANOVA Table for PDR in a 100 m Direct Line-of-Sight Scenario

Parameters	DOF	SS	MS	F	Contribution
TP	5	82.94	16.59	1.25	17.7%
AG	2	93.44	46.72	3.53	50.1%
ST	2	60.11	30.06	2.27	32.2%
Error	8	105.78	13.22		
Total	17	342.28			100%

TP = Transmit power, AG = Antenna gain, and ST = Surrounding temperature

Table 12

ANOVA Table for Average RSSI in a 100 m Direct Line-of-Sight Scenario

Parameters	DOF	SS	MS	F	Contribution
TP	5	686.67	137.33	14.27	5.7%
AG	2	4510.33	2255.17	234.3	93.2%
ST	2	52	26	2.7	1.1%
Error	8	77	9.63		
Total	17	5326			100%

TP = Transmit power, AG = Antenna gain, and ST = Surrounding temperature

In a 100 m direct line-of-sight environment, the most significant parameter that affects the PDR and average RSSI is the antenna gain, with an impact ratio of 50.1% and 93.2%, respectively. However, the ranking parameters are different compared to the 1 km one. In terms of PDR, the ranking order is determined as antenna model > surrounding temperature > TP, whereas for the average RSSI, antenna model > TP > surrounding temperature is the ranking order. There is a conflict in terms of the ranking order of the parameters obtained

from the Taguchi and ANOVA analysis. The reason behind this might be the 100 m communication range, which is considered insufficient in distinguishing and analyzing the performance of 2 dBi and 5 dBi antennas. As shown in Table 4 and Figure 4(b), the PDRs acquired from the 2 dBi and 5 dBi antennas at all experimental trials are the same, and the difference in terms of the average RSSI is also very small. Therefore, it is recommended that the reliability of LoRa communication be tested at a longer communication range, such as 500 m, to properly determine the order of the importance of parameters. However, findings obtained from experimental work in a 100 m environment are still useful. It was discovered that the minimum TP (5 dBm) for the 2 dBi antenna yields the same PDR as the 5 dBi antenna, regardless of the surrounding temperature.

Based on the Taguchi and ANOVA analysis performed, it was discovered that the TP could be reduced to as low as 15 dBm for a maximum PDR in a 1 km direct line-of-sight environment if the 5 dBi antenna is used. Therefore, by applying Equations 8 and 9, the LoRa power consumption can be reduced by approximately 168.4 mW, and the maximum number of data transmissions is increased to 6289 times, which is more than double the data that can be transmitted using the default TP (2500 times). For the 100 m direct line-of-sight scenario, applying the lowest TP (5 dBm) on the 2 dBi antenna can still yield maximum PDR while at the same time reducing the power consumption by up to 196.8 mW and transmitting about 17388 more data compared to default TP. Although it was discovered that the 5 dBi performs better in terms of PDR and average RSSI, in most UAV applications, the UAV will perform more than hovering and most likely not stay in the effective coverage angle of the 5 dBi antenna. Thus, it is recommended that the 2 dBi antenna be applied in UAV-based LoRa applications as the antenna has a 360° coverage angle, making the UAV not limited by maneuverability.

In the future, additional parameters such as BW, SF, and CR can be included in the Taguchi and ANOVA analysis to determine the optimum LoRa configuration for further minimizing the power consumption. Also, the performance of a 3.5 dBi antenna model can be evaluated, and the surrounding temperature can be further varied by introducing a colder (less than 10°C) and hotter environment (more than 40°C). Further analysis can be conducted to examine the impact of other factors on the performance of UAV-based LoRa communication, such as antenna gain, weight, and coverage capability. Additional experiments will also be conducted to assess the performance of each antenna at intermediate distances between 100 m and 1000 m.

CONCLUSION

The application of UAVs can increase LoRa's potential, especially in monitoring and precision agriculture. Many parameters can affect the performance of the UAV-based LoRa communication network, such as TP, BW, SF, CR, and surrounding temperature. The

main contribution of this study is the investigation of the optimum LoRa configuration, which consists of TP, antenna model, and the surrounding temperature. It aims to achieve maximum PDR and RSSI with less power consumption. Two different statistical methods (Taguchi and ANOVA) are applied to determine the ranking order of these parameters. In a 1 km direct line-of-sight environment, results from both Taguchi and ANOVA analysis are in agreement that the most significant parameter is the antenna model, followed by TP and surrounding temperature. The optimum LoRa configuration for the best PDR is TP = 15 dBm, antenna model = 5 dBi antenna, and surrounding temperature = 34°C, reducing the power consumption by approximately 168.4 mW. For a 100 m communication range, the TP can be set to as low as 5 dBm on the 2 dBi antenna, reducing the power consumption by up to 196.8 mW and transmitting 17388 times more data compared to the default configuration. Meanwhile, in a 1 km communication range, the proposed work's efficacy in the maximum number of data transmissions is approximately 151.56% higher than that of the default setting. Minimizing power consumption is essential so that a lighter power supply can be equipped, prolonging the flight time of the UAV. In the future, the reflection signal from the UAV that will affect the antenna performance can be calculated and investigated.

ACKNOWLEDGEMENT

This work was supported by Collaborative Research in Engineering, Science, and Technology (CREST) with grant no. 304/PELECT/6050424/C121.

REFERENCES

- Bademlioglu, A. H., Canbolat, A. S., Yamankaradeniz, N., & Kaynakli, O. (2018). Investigation of parameters affecting Organic Rankine Cycle efficiency by using Taguchi and ANOVA methods. *Applied Thermal Engineering*, 145(1), 221–228. <https://doi.org/10.1016/j.applthermaleng.2018.09.032>
- Behjati, M., Noh, Y., Alobaidy, H. A. H., Zulkifley, M. A., Nordin, R., & Abdullah, N. F. (2021). LoRa communications as an enabler for internet of drones towards large-scale livestock monitoring in rural farms. *Sensors*, 21(15), 5044–5071. <https://doi.org/10.3390/s21155044>
- Caruso, M., Boano, C. A., & Romer, K. (2021). Collection of data with drones in precision agriculture: Analytical model and LoRa case study. *IEEE Internet of Things Journal*, 8(22), 16692–16704. <https://doi.org/10.1109/JIOT.2021.3075561>
- Cattani, A., Chessa, S., Escolar, S., Barba, J., & Lopez, J. C. (2017). An experimental evaluation of the reliability of lora long-range low-power wireless communication. *Journal of Sensors and Actuator Networks*, 6(2), 7–26. <https://doi.org/10.3390/jsan6020007>
- Davis, R., & Pretesh, J. (2018). Application of Taguchi-based design of experiments for industrial chemical processes. In V. Silva (Ed.), *Statistical Approaches With Emphasis on Design of Experiments Applied to Chemical Processes* (pp. 137-156). IntechOpen. <http://dx.doi.org/10.5772/intechopen.69501>

- Ding, Y., Feng, Y., Lu, W., Zheng, S., Zhao, N., Meng, L., Nallanathan, A., & Yang, X. (2022). Online edge learning offloading and resource management for UAV-assisted MEC secure communications. *IEEE Journal of Selected Topics in Signal Processing*, 17(1), 54–65. <https://doi.org/10.1109/JSTSP.2022.3222910>
- Edward, P., El-Aasser, M., Ashour, M., & Elshabrawy, T. (2020). Interleaved chirp spreading LoRa as a parallel network to enhance LoRa capacity. *IEEE Internet of Things Journal*, 8(5), 3864–3874. <https://doi.org/10.1109/JIOT.2020.3027100>
- Faber, M. J., van der Zwaag, K. M., dos Santos, W. G. V., de O Rocha, H. R., Segatto, M. E. V., & Silva, J. A. L. (2020). A theoretical and experimental evaluation on the performance of LoRa technology. *IEEE Sensors Journal*, 20(16), 9480–9489. [10.1109/JSEN.2020.2987776](https://doi.org/10.1109/JSEN.2020.2987776)
- Ghazali, M. H. M., Teoh, K., & Rahiman, W. (2021). A systematic review of real-time deployments of UAV-based LoRa communication network. *IEEE Access*, 9, 124817–124830. <https://doi.org/10.1109/ACCESS.2021.3110872>
- Ginting, E., & Tambunan, M. M. (2018). Selection of optimal factor level from process parameters in palm oil industry. In *IOP Conference Series: Materials Science and Engineering* (Vol. 288, No. 1, p. 012056). IOP Publishing. <https://doi.org/10.1088/1757-899X/288/1/012056>
- Liang, R., Zhao, L., & Wang, P. (2020). Performance evaluations of LoRa wireless communication in building environments. *Sensors*, 20(14), 3828–3847. <https://doi.org/10.3390/s20143828>
- Liu, J., Wu, J., & Liu, M. (2020). UAV monitoring and forecasting model in intelligent traffic oriented applications. *Computer Communications*, 153, 499–506. <https://doi.org/10.1016/j.comcom.2020.02.009>
- Liu, S., Yang, X., & Zhou, Z. (2020). Development of a low-cost UAV-based system for CH₄ monitoring over oil fields. *Environmental Technology*, 42(20), 3154–3163. <https://doi.org/10.1080/09593330.2020.1724199>
- Lu, W., Yandan, M., Feng, Y., Gao, Y., Zhao, N., Wu, Y., & Moose, P. H. (2022). Secure transmission for multi-UAV-assisted mobile edge computing based on reinforcement learning. *IEEE Transactions on Network Science and Engineering*, 10(3), 1270–1282. <https://doi.org/10.1109/TNSE.2022.3185130>
- Petajajarvi, J., Mikhaylov, K., Pettisalo M., Janhunen, J., & Iinatti, J. (2017). Performance of a low-power wide-area network based on LoRa technology: Doppler, robustness, scalability, and coverage. *International Journal of Distributed Sensor Networks*, 13(3), 1–16. <https://doi.org/10.1177/1550147717699412>
- Said, M. S. M., Ghani, J. A., Kassim, M. S., Tomadi, S. H., & Haron, C. H. C. (2013). Comparison between Taguchi method and response surface methodology (RSM) in optimizing machining condition. In *Proceeding of 1st International Conference on Robust Quality Engineering* (pp. 60-68). UTM Razak School.
- Sanchez-Iborra, R., Sanchez-Gomez, J., Ballesta-Vinas, J., Maria-Dolores, C., & Skarmeta, A. F. (2018). Performance evaluation of LoRa considering scenario conditions. *Sensors*, 18(3), 772–791. <https://doi.org/10.3390/s18030772>
- Trasvina-Moreno, C. A., Blasco, R., Marco, A., Casas, R., & Trasvina-Castro, A. (2017). Unmanned aerial vehicle based wireless sensor network for marine coastal environment monitoring. *Sensors*, 17(3), 460–482. <https://doi.org/10.3390/s17030460>

- Vlasceanu, E., Dima, M., Popescu, D., & Ichim, L. (2019). Sensor and communication considerations in UAV-WSN based system for precision agriculture. In *2019 IEEE International Conference on Cybernetics and Intelligent Systems (CIS) and IEEE Conference on Robotics, Automation and Mechatronics (RAM)* (pp. 281-286). IEEE Publishing. <https://doi.org/10.1109/CIS-RAM47153.2019.9095823>
- Wang, S. Y., Chen, Y. R., Chen, T. Y., Chang, C. H., Cheng, Y. H., Hsu, C. C., & Lin, Y. B. (2017). Performance of LoRa-based IoT applications on campus. In *2017 IEEE 86th vehicular technology conference (VTC-Fall)* (pp. 1-6). IEEE Publishing. <https://doi.org/10.1109/VTCFall.2017.8288154>
- Wang, Z., Wen, M., Dang, S., Yu, L., & Wang, Y. (2021). Trajectory design and resource allocation for UAV energy minimization in a rotary-wing UAV-enabled WPCN. *Alexandria Engineering Journal*, *60*(1), 1787–1796. <https://doi.org/10.1016/j.aej.2020.11.027>
- Yim, D., Chung, J., Cho, Y., Song, H., Jin, D., Kim, S., Ko, S., Smith, A., & Riegsecker, A. (2018). An experimental LoRa performance evaluation in tree farm. In *2018 IEEE sensors applications Symposium (SAS)* (pp. 1-6). IEEE Publishing. <https://doi.org/10.1109/SAS.2018.8336764>
- Zorbas, D., & O'Flynn, B. (2019). A network architecture for high volume data collection in agricultural applications. In *2019 15th International Conference on Distributed Computing in Sensor Systems (DCOSS)* (pp. 578-583). IEEE Publishing. <https://doi.org/10.1109/DCOSS.2019.00107>

